Journal of
Water & Climate Change

IWA PUBLISHING

Journal of Water and Climate Change Vol 15 No 5, 2110 doi: 10.2166/wcc.2024.549

Assessment of climate change impacts on rainfall and streamflow in the Alto Paranapanema Basin, Brazil

André Teixeira da Silva Hucke [a], Mateus Nardini Menegaz [b], Jorge Manuel Guieiro Pereira Isidoro [c,d] and Rafael de Oliveira Tiezzi [a,b,e,*]

[a] Postgraduate Program in Environmental Science and Engineering, Federal University of Alfenas, Rodovia José Aurélio Vilela, 11999 (BR 267 Km 533), Cidade Universitária, Poços de Caldas, MG CEP 37715-400, Brazil
[b] Postgraduate Program in Environmental Science, Federal University of Alfenas, Rua Gabriel Monteiro da Silva, 700, Centro – Alfenas, MG, CEP: 37130-001 CEP 37715-400, Brazil
[c] Department of Civil Engineering, Institute of Engineering, University of Algarve, Campus da Penha, 8005-139 Faro, Portugal
[d] MARE – Marine and Environmental Sciences Centre/ARNET – Aquatic Research NETwork, Rua da Matemática, 49, 3004-517 Coimbra, Portugal
[e] Nature Center Science, University Federal of São Carlos, Campus Lagoa do Sino, Lauri Simões de Barros Road, km 12 – SP-189, Aracaçu, Buri, SP, Brazil
*Corresponding author. E-mail: rafaeltiezzi@ufscar.br

ATdSH, 0000-0001-8565-8191; JMGPI, 0000-0002-6901-5652; RdOT, 0000-0001-8682-7807

ABSTRACT

Climate change has the potential to fundamentally transform landscapes on global scale. Leveraging advanced predictive modeling to enhance water resource management within the Alto Paranapanema Basin (Brazil), holds the potential to proactively anticipate challenges and alleviate the impacts and conflicts arising from this phenomenon. This is particularly important in a region boasting over 1,600 centerpivot irrigation systems. This study employs the Soil Moisture Accounting Procedure, a physical model, to simulate long-term climate datasets and flows. Future climate scenarios, rooted in the Representative Concentration Pathways, are developed through the downscaling of Global Climate Models. The findings reveal a temporal shift in rainfall patterns, characterized by a reduction during the wet season of up to 40% compared to the average historical rainfall, and an increase throughout the dry season up to 40% compared to the same historical, estimated by the Eta -BESM model. These changes present challenges regarding to water availability, hydroelectric generation, and agricultural. By fostering collaboration among different governmental entities responsible for the managements of basins and harnessing the potential of predictive models, this research advocates for the adoption of proactive strategies in management of water resources. These strategies are imperative to effectively counteract the far-reaching effects of climate change.

Key words: Alto Paranapanema, climate change, Soil Moisture Accounting Procedure (SMAP), streamflow, water resources

HIGHLIGHTS

- Impacts of climate change, with four Regional Climate Models and two Representative Concentration Pathways, in rainfall and river flow utilizing Soil Moisture Accounting Procedure as an analytical tool.
- Watershed has a major impact on society around the river and downstream.
- River flow changes could disrupt energy and water for those communities.

GRAPHICAL ABSTRACT

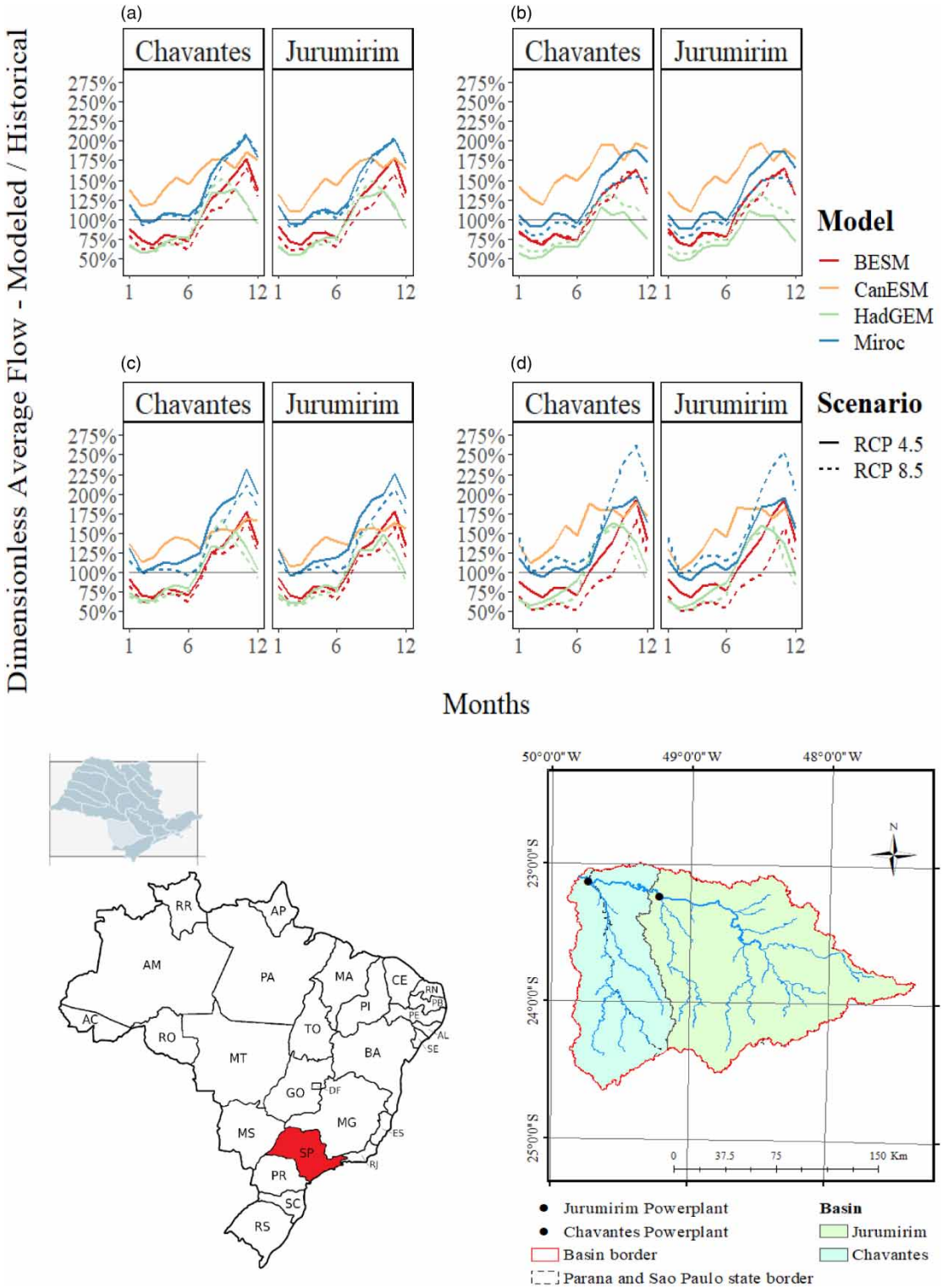

INTRODUCTION

The latest Assessment Report (AR6) published by the Intergovernmental Panel on Climate Change (IPCC) in August 2021 unequivocally indicates that human influence is responsible for the rapid pace of climate change, exceeding what would – otherwise – occur naturally. The report confirms that greenhouse gasses emitted from human activities are the main culprit for climate change (IPCC, 2021). The impacts of climate change are widespread and diverse, ranging from rising sea levels and altered rainfall patterns to changes in evapotranspiration and energy supply in nations heavily reliant on hydroelectric power. In addition, climate change poses a significant threat to food security (Zhang *et al.* 2018).

The relationship between human activity and climate prediction dates to the origin of agriculture, which marked the first large-scale food supply for humanity and was essential for population growth and technological development (Commoner 2020). However, nowadays, the planet faces significant disruptions to its ecosystems, and there are important questions regarding the maximum population it can sustain. In the early days of agriculture, people viewed the seasons as milestones to determine when to plant different crops and how long food stores would last. Today, this concept of carefully observing the climate behavior is more relevant than ever, as human activity is heavily dependent on water resources, and climate change is altering the spatial and temporal distribution of rainfall. While modern climate prediction requires advanced supercomputers, it remains as essential as it was for our ancestors (Jackson *et al.* 2001).

The complexity of climate, including the multiple factors that influence weather patterns and climate change, makes accurate prediction remarkably difficult (Gueymard 2012). However, statistical models offer a means of predicting climate trends by analyzing historical data, despite inherent uncertainties. One useful tool for climate prediction is the stochastic climate generator, which can simulate hydrological series based on historical data. To assess the effectiveness of such simulations, several common methods are employed to determine the degree of statistical correlation with historical data, such as the Nash–Sutcliffe efficiency (NSE) model coefficient.

Global Climate Models (GCMs) are computer simulations used to predict how the climate will respond to future changes (Chou *et al.* 2014a, 2014b). The outputs of GCMs can be incorporated as inputs to stochastic models, which can generate projections based, e.g., on the IPCC Representative Concentration Pathways (RCPs), indicating how much greenhouse gas emissions are expected to increase (van Vuuren *et al.* 2011). GCMs are generated and provided by several institutions, including the Canadian Centre for Climate Modelling and Analysis (CCCma), the Center for Climate System Research (CCSR), the National Institute of Space Research (INEP), and the Met Office Hadley Centre. To improve their accuracy, GCMs can also be downscaled or regionalized by incorporating additional variables, such as topography, land use, or local climate data that are specific to the region under analysis. In Brazil, the regionalization process is performed by the National Institute for Space Research (INPE), which uses multiple GCMs to better represent and understand possible future climate scenarios in the Brazilian territory (Chou *et al.* 2014b).

Simulating long-term climate datasets for a specific region and altering its initial conditions is a feasible approach to understand the impact of climate change on future rainfall, evapotranspiration, and river flow (Maraun *et al.* 2010; Green *et al.* 2011). To this end, in Brazil, hydrologists widely employ the Soil Moisture Accounting Procedure (SMAP) model, which utilizes rainfall and evapotranspiration data to derive river flow. The SMAP model generates both unit runoff values, a measure of the watershed's water production per unit area, and total river flow discharge (Barros *et al.* 2009). Further details on SMAP can be found in Lopes (1999) and Tiezzi *et al.* (2018, 2019).

The relationship between rainfall and runoff is highly nonlinear and depends on specific watershed characteristics, such as land use and basin topography. The interconnection between different sub-basins has a significant influence on the river flow downstream, as the runoff from upstream watersheds affects the river flow in the watersheds downstream, a phenomenon named as incremental watersheds. It is well known that although headwater watersheds are located miles away upstream, they can significantly impact the quantity and quality of water downstream along the river path (Skaggs *et al.* 1994).

The aim of this study was to investigate the potential impacts of climate change on rainfall and river flow in two key watersheds, Jurumirim and Chanvantes. These watersheds play a critical role in supplying water to cities in the Avare region, besides their importance for the local economy, including tourism and property values around the reservoir. Climate change can significantly alter hydrologic processes in the watersheds, which in turn can affect communities along the river, disrupt electricity generation in hydroelectric plants, and impact agriculture and livestock practices in the region. Furthermore, these changes can have a ripple effect throughout all connected rivers. Despite the abundance of research on the impacts of climate change on hydrological systems, few studies have incorporated such many climate models and scenarios for basins with a major impact on society, as is the case in this study.

ALPA Basin characteristics

In Brazil, one of the major headwater watersheds for hydroelectric generation is the Alto Paranapanema (ALPA) Basin, in the State of São Paulo. The Rio Paranapanema, in which the ALPA is the main headwater sub-basin, has 11 hydroelectric power plants located in this basin with a total output of 2.4 GW. This basin is also one of the major tributaries of the Parana River, that leads to the Itaipu dam, the second biggest hydroelectric power plant in the world regarding installed capacity (14 GW).

Another major feature of the ALPA is its agricultural potential. The ALPA has the highest center-pivot irrigation system count of all sub-basins in the State of Sao Paulo (over 1,600 in 2017), with a major increase through the years, as shown in Figure 1. This number of center-pivot irrigation system strongly contributes for the ALPA sub-basin region to have the highest Gross Domestic Product (GDP) in the state of São Paulo, where the agriculture sector corresponds to 14% of its GDP, split by 20% in livestock and 80% in farming (Barros *et al.* 2021). In 2022, the State of Sao Paulo was responsible for around 25% of Brazil's GDP (IBGE 2023).

The methodology adopted for this study was based on previous research carried out in the ALPA Basin by Tiezzi *et al.* (2018) and Tiezzi *et al.* (2019). The ALPA basin covers an area of 22,689 km^2, with an average elevation of 610 meters, and is home to major industrial, agricultural, and livestock sites. However, according to SIGRH (2023), only 4,677 km^2 of the area was still covered by natural forests in 2023, and this is unfortunately expected to continue diminishing. The basin spans across the São Paulo and Paraná state limits, as depicted in Figure 2. To analyze the impacts of climate change in the region, the basin was divided into two sub-basins, with the first sub-basin's outlet located in the Jurumirim reservoir and the second sub-basin's outlet located in the Chavantes reservoir. Rainfall data generated by ETA/INEP, containing all GCM components, were used for all the counties within the basin.

The Chavantes power plant has a production capacity of 414 MW and a reservoir area of 428.34 km^2, while the Jurumirim power plant has a production capacity of 100.96 MW and a reservoir of 449 km^2. It is worth noting that the water flowing through this basin comes from the Paranapanema River and the Itararé River, and it plays a crucial role in regulating water resources in the region.

MATERIALS AND METHODS

GCMs and Regional Climate Models

GCMs are simulated by several research institutions around the world, each using their own models. GCMs used in this study were run with greenhouse gas emissions projected by the IPCC Fifth Assessment Report. The grid size for these models typically ranges from 400 × 400 km to 200 × 200 km. The Regional Climate Models (RCMs), like the Eta model, takes the GCM and focuses computational efforts to improve the output data. Table 1 summarizes the main features of the GCM models used in this study (BESM, CanESM2, HadGEM2-EM, Miroc5).

The Eta model has been adapted to facilitate downscaling, which involves regionalizing GCMs on a more precise scale, tailored to the Central and South American regions. It has been utilized by CPTEC/INPE for climatological and meteorological forecasts since 1997. Starting from 2010, this model was also employed for studying climate change driven by global models. The Eta model incorporates the annual dynamics of the microphysical vegetation cycle of clouds, a convective cloud scheme, and short- and long-wave balance at a constant CO_2 concentration (Chou *et al.* 2014a, 2014b).

The GCMs used in this study (see Table 1) were selected as these were the only four GCMs regionalized using the Eta model. These models were coupled resulting in four variants: Eta–BESM, Eta–CanESM, Eta–HadGEM2-ES, and Eta–Miroc5. Precipitation and evapotranspiration data spanning the period from 1960 to 1989, as well as projections up to 2,100 based on RCPs, were obtained using these models. The Eta model employs a vertical resolution of 38 levels and a spatial resolution of 20 km (Chou *et al.* 2014a). It is important to clarify that although the Eta models generate a significant amount of data, only precipitation and evapotranspiration were considered for modeling the rainfall–runoff process in this study.

Representative Pathways Scenarios

RCP 4.5 and 8.5 were the scenarios employed for the different regionalized Eta models, as they represent the best- and worst-case scenarios projected by the IPCC. The RCP 4.5 scenario represents a radiative forcing level, or energy balance in the atmosphere, caused by human activity of 4.5 W/m^2, and is a stabilization scenario. The RCP 8.5 scenario represents a high emissions scenario, with a radiative forcing level of 8.5 W/m^2 (IPCC, 2021). The RCP 2.6 scenario was omitted from

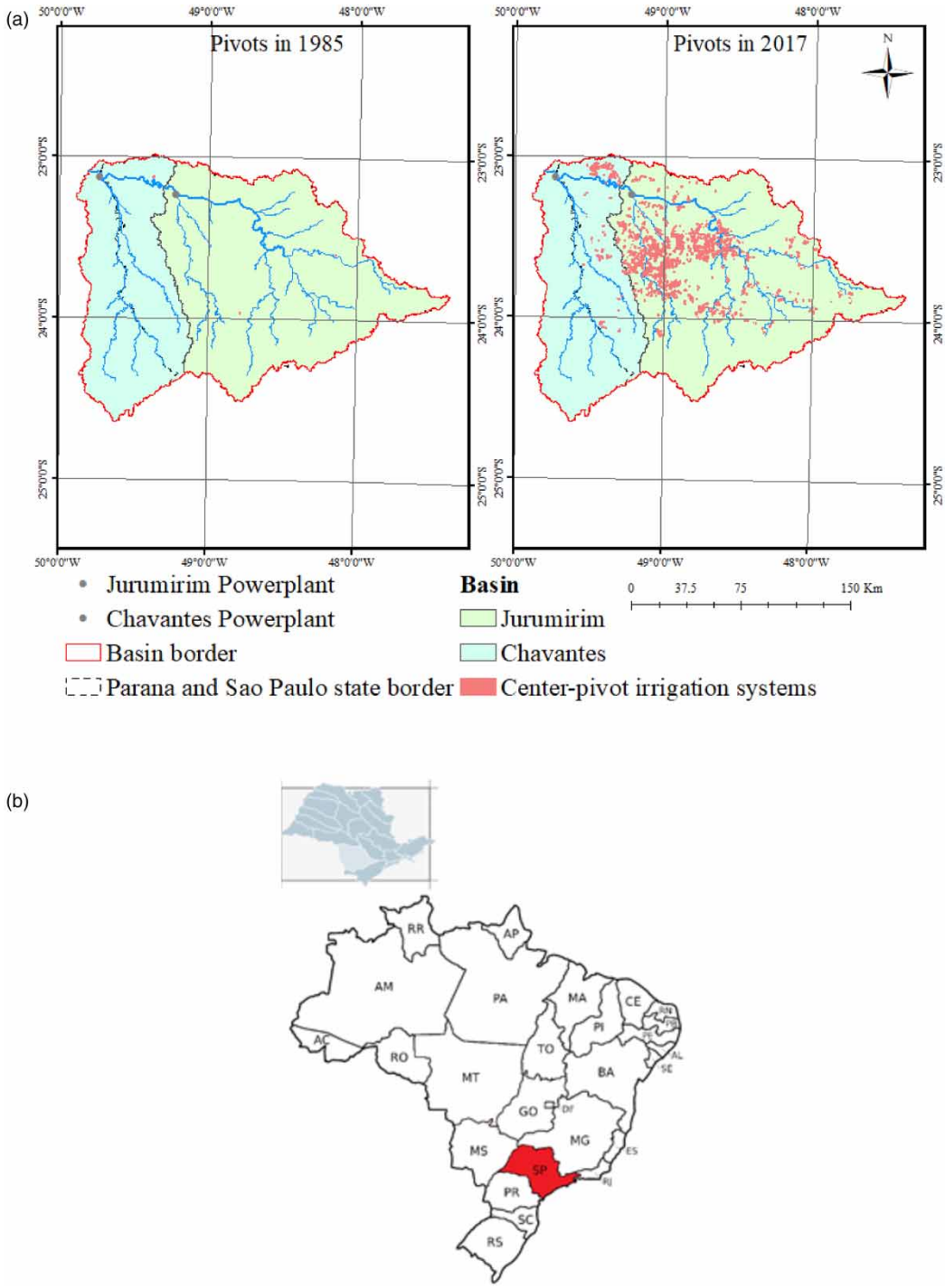

Figure 1 | (a) Increase in center-pivot irrigation systems around the main rivers and powerplants on the delimited ALPA region between 1985, with just three center-pivot irrigation systems, and with over 1,600 pivots in 2017 (Santos *et al.* 2023). (b) Location of ALPA basin, state of São Paulo, Brazil. The figure on the top of Brazil's map shows the delimitation of the most important sub-basins in the state of São Paulo. *Source:* Adapted from SigRH (2023).

this study due to its projected imminent occurrence. The primary objective of this study is to examine the potential ramifications if the scenarios deteriorate. Likewise, the RCP 6.0 scenario was not employed to concentrate solely on the extreme cases and streamline the analysis process.

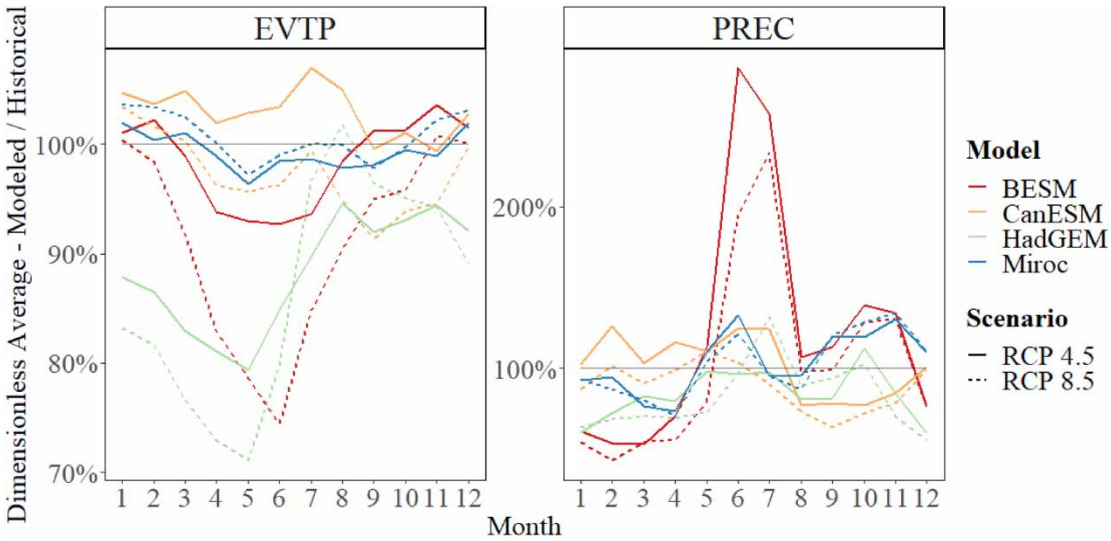

Figure 2 | Dimensionless average of monthly evapotranspiration (left) and rainfall (right) for ALPA, in comparison to historical rainfall, from 2010 to 2099. The results are based on four different climate models: Eta–BESM, Eta–CanESM, Eta–HadGEM, and Eta–Miroc, and two IPCC scenarios: RCP 4.5 and RCP 8.5.

Table 1 | Main characteristics of the GCMs used in this study

Model	Institution	Resolution (lat° × long°)	Levels	Vegetation	Addition information
BESM	National Institute for Space Research, Brazil	0.25–2° × 1°	28 Terrestrial and 50 oceanic	12 Different types	Radioactive interactions and convective cloud system
CanESM2	Canadian Center for Climate Modeling and Analysis, Canada	2.8125° × 2.8125°	35 Atmospheric	Nine different types in three different vegetative systems	Carbon cycle components and dead organic matter
HadGEM2-EM	Met Office Hadley Center, United Kingdom	1.875° × 1.25°	38 Atmospheric	Five different types	Model with atmospheric chemistry with aerosols
Miroc5	Japan Agency for Marine-Earth Science and Technology, Atmosphere and Ocean Research Institute, Japan	1.41° × 1.41°	40 Terrestrial and 50 oceanic	Three groups	Uses albedo of snow and water mirrors. Also uses clouds microphysics

Statistical analysis and model calibration

To enhance the accuracy of the models employed in this study, a meticulous calibration process was undertaken using historical data obtained from sound sources such as the Brazilian National Water Agency (ANA) and the Brazilian National System Operator (ONS). Typically, historical series spanning a period of five to ten years are used to convert rainfall into streamflow through the application of a numerical simulation model. In this study, the SMAP model was specifically adopted for this purpose. This model has been extensively used in previous research and has undergone validation in multiple studies (e.g., Barros *et al.* 2009; O'Neill *et al.* 2010; Zhang & Zhou 2016; Wigneron *et al.* 2017; Peng *et al.* 2021). The SMAP model operates by calculating flow based on precipitation and evaporation and is classified as a lumped parametric model and is based on the Standard Watershed IV model and on the Mero model. SMAP was originally developed for daily data, and later updated to handle hourly and monthly data (Lopes 1999). This study uses the monthly version of the SMAP model. SMAP was developed by Lopes *et al.* (1982) and was presented at the International Symposium on Rainfall–Runoff Modeling that took place at Mississippi State University (USA). To optimize the model's performance, the NSE coefficient (Nash & Sutcliffe 1970) was selected as the optimization criterion (employing Excel's SOLVER function).

RESULTS AND DISCUSSION

The dimensionless average monthly rainfall for the RCP 4.5 and 8.5 scenarios, as well as the four different climate models (Eta–BESM, Et-CanESM, Eta–HadGEM and Eta–Miroc), from 2010 to 2099 are presented in Figures 3–6. The dimensionless average is represented as a percentage, with values above the 100% mark indicating increases and values below indicating reductions. The results were obtained by comparing the calculated rainfall against ALPA's historical rainfall data from 1931 to 2018. Most models indicate a decrease in rainfall from December to April, and an increase in rainfall from May to July. However, the months from August to November do not show any clear signal when comparing the different models. It is also worth noting that the Eta–BESM model is considered the best representative model for the ALPA region (Chou *et al.* 2014a, 2014b), as it indicates a shift in rainfall throughout the year. Specifically, this model shows that the dry months, June, July, and August, experience an increase in rainfall, whereas the wet months of October through April, have a potential increase in extreme rainfall events. While it is true that the Eta–BESM model shows an increase in rainfall

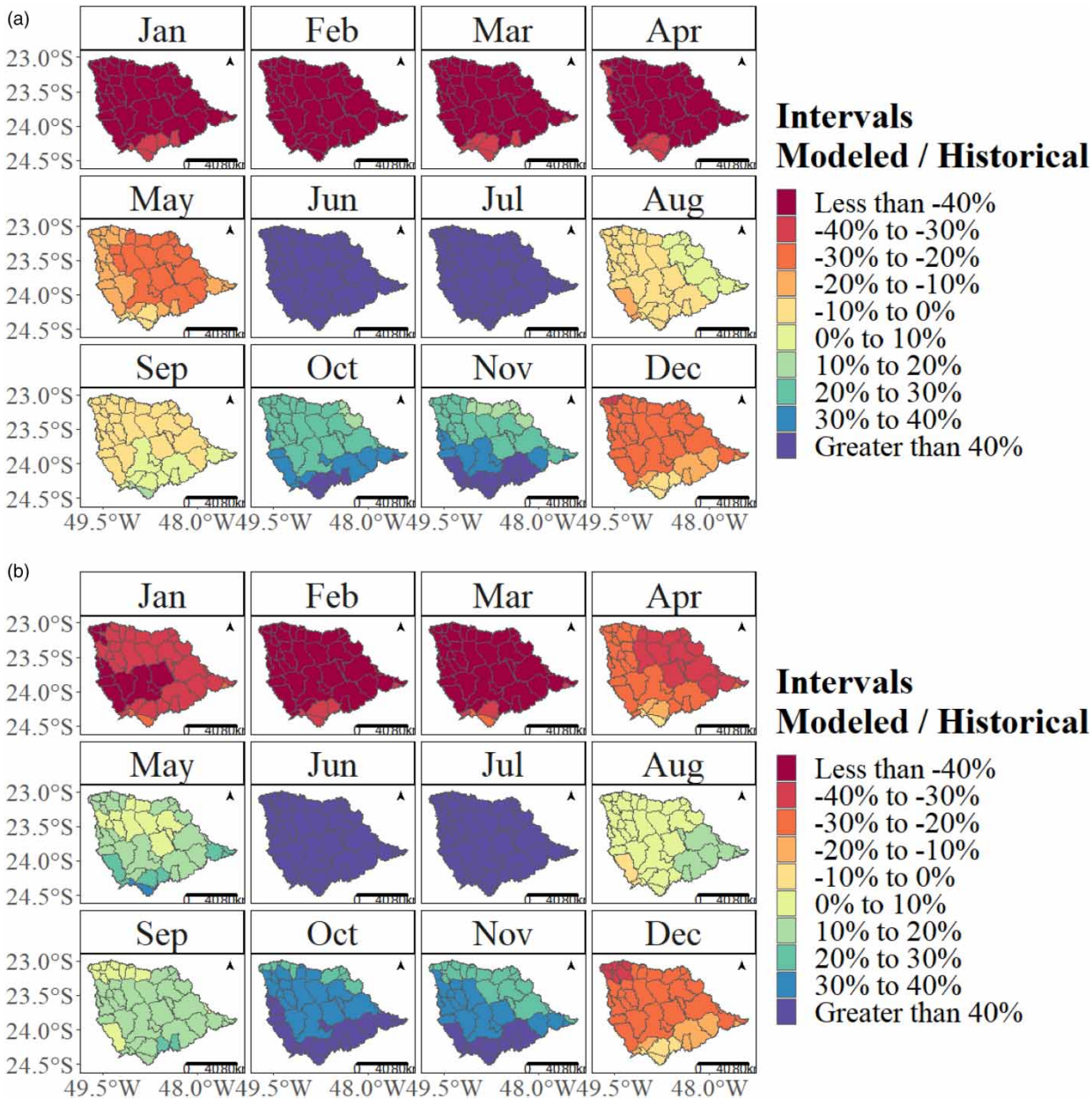

Figure 3 | Yearly rainfall variation for the Eta–BESM climate model under the RCP 4.5 (a) and RCP 8.5 (b) scenarios.

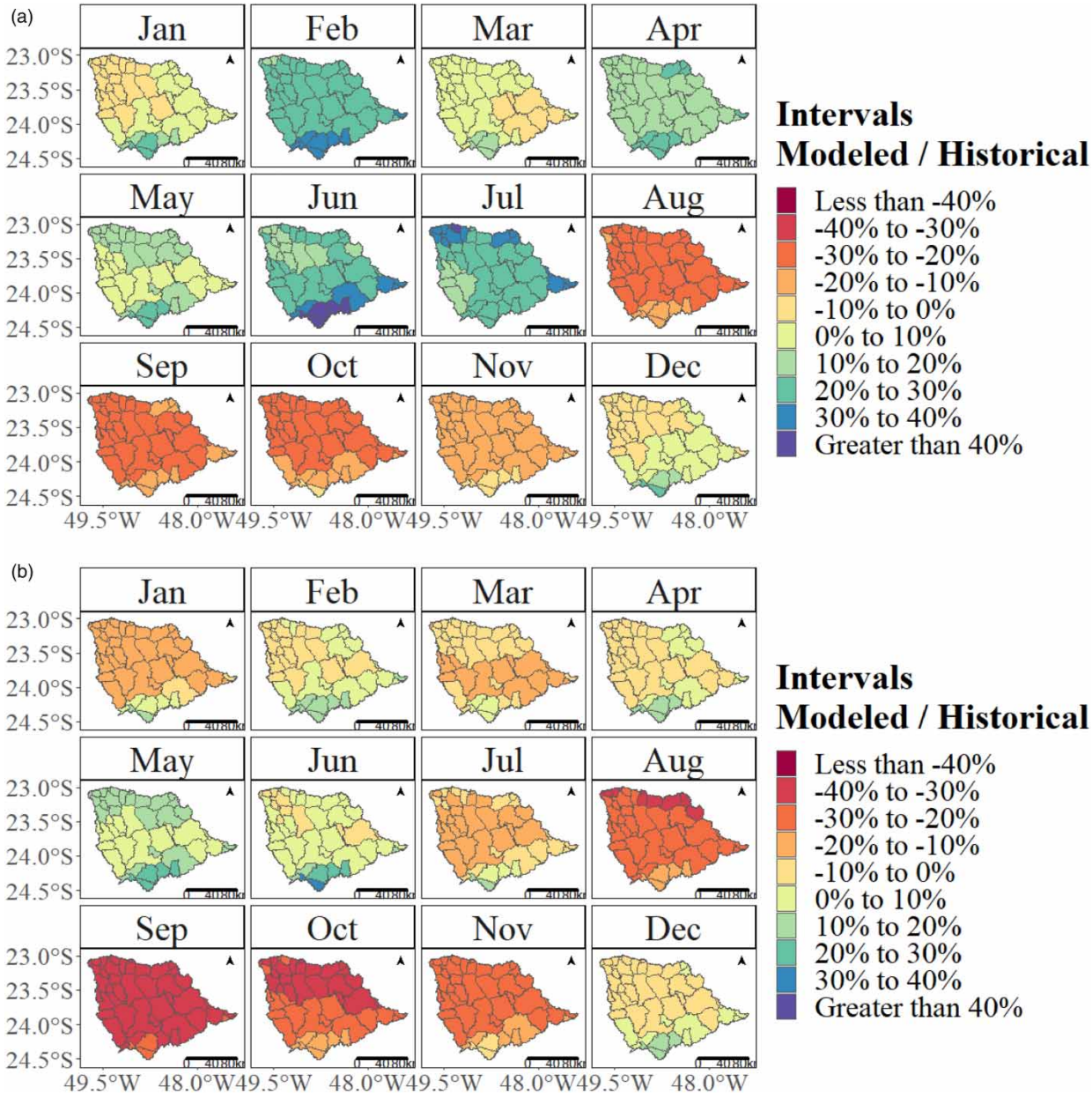

Figure 4 | Yearly rainfall variation for the Eta–CanESM climate model under the RCP 4.5 (a) and RCP 8.5 (b) scenarios.

in dry months, other models agree that the dry months become even drier, while the wet months may become more extreme. Figure 3 shows a greater loss of water due to evapotranspiration and soil water evaporation. The data obtained from this first analysis can then be utilized in statistical models, such as SMAP, which will output a predicted river flow measurement.

To ensure an accurate interpretation of the dimensionless average analysis, it is fundamental to consider the potential for misinterpretation. For instance, if we consider a dry period with a historical average rainfall of 10 mm and a model indicating an additional 10 mm of rainfall, the total rainfall would be 20 mm. Using dimensionless average analysis, this increase would be calculated as 100%, with the resulting line reaching 200%. This dramatic increase has a strong visual impact and can bias the interpretation of the data. However, in a wet period with a rainfall depth of 200 mm, the same model showing a 10 mm increase would only result in a dimensionless average increase of 5%, i.e., a minimal change. In both hypothetical scenarios, the increase in (absolute) rainfall volume is the same, but the historical (relative) data differs. To avoid misinterpretation, special attention should be paid to the dry season from May through August, where base precipitation values can be very low.

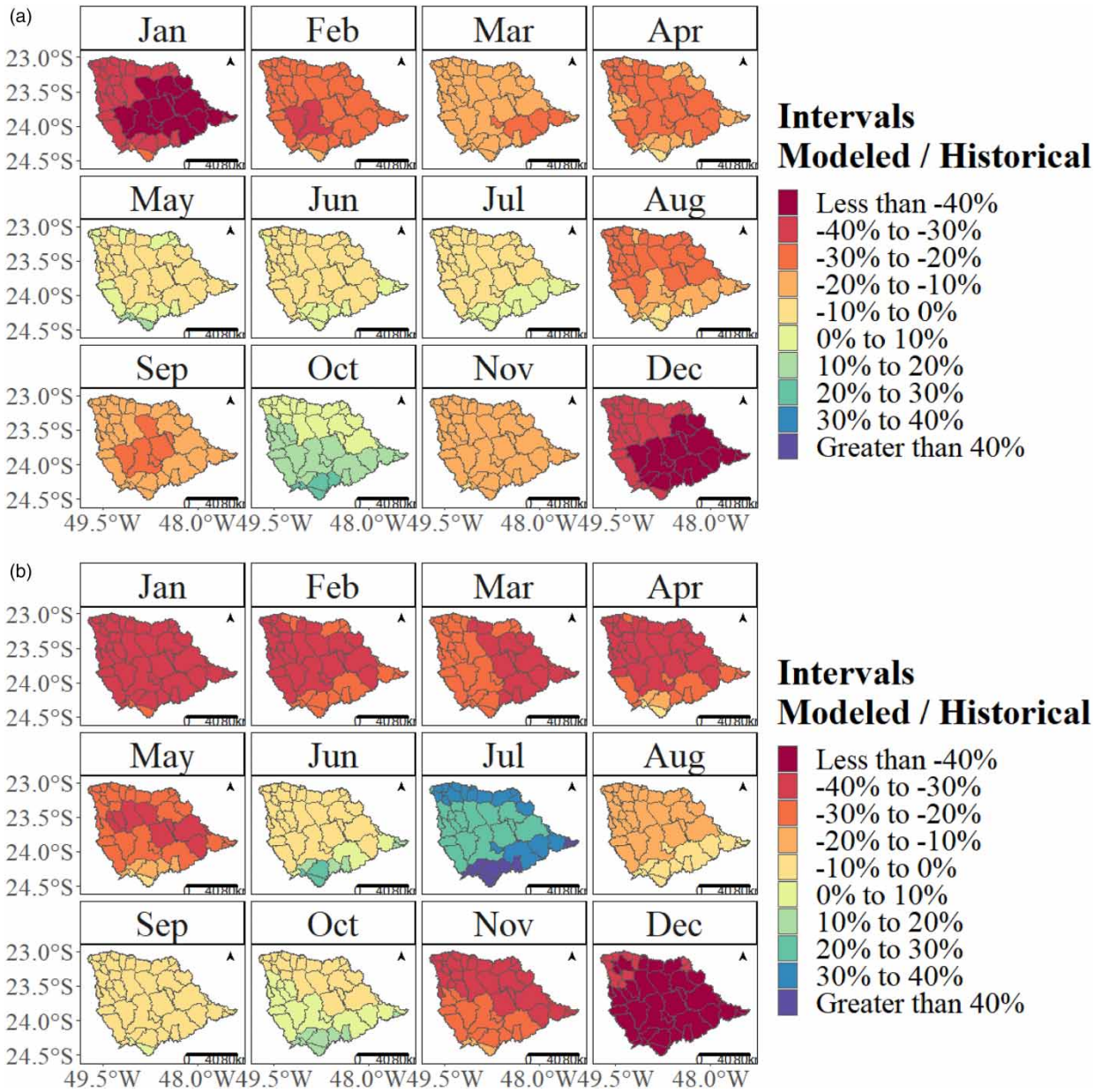

Figure 5 | Yearly rainfall variation for the Eta–HadGEM climate model under the RCP 4.5 (a) and RCP 8.5 (b) scenarios.

The data presented can be further disaggregated by counties. To minimize the variability in climate models and identify trends in rainfall and its impacts for the next 100 years, the analysis was conducted on distinct scenarios and models. Figure 3(a) and 3(b) displays the results of Eta–BESM RCP 4.5 and RCP 8.5 models, respectively. Figure 4(a) and 4(b) shows the outcomes of Eta–CanESM RCP 4.5 and RCP 8.5 models. Similarly, Figure 5 illustrates the results of Eta–HadGEM RCP 4.5 and RCP 8.5 models, while Figure 6 displays the findings of Eta–Miroc RCP 4.5 and RCP 8.5 models. In these figures, warm colors such as red and yellow indicate a reduction in rainfall, while cold colors, such as blue and green, represent an increase in rainfall.

According to Figure 4, there is a noticeable increase of hydrological stress in the region under analysis. This is clear from the reduction in rainfall during the months of January to April. Additionally, the results indicate an increase in rainfall during June and July, which are months of the dry season, and during October and November, which are months of the wet season. This pattern emphasizes the shift in rainfall regime due to climate change.

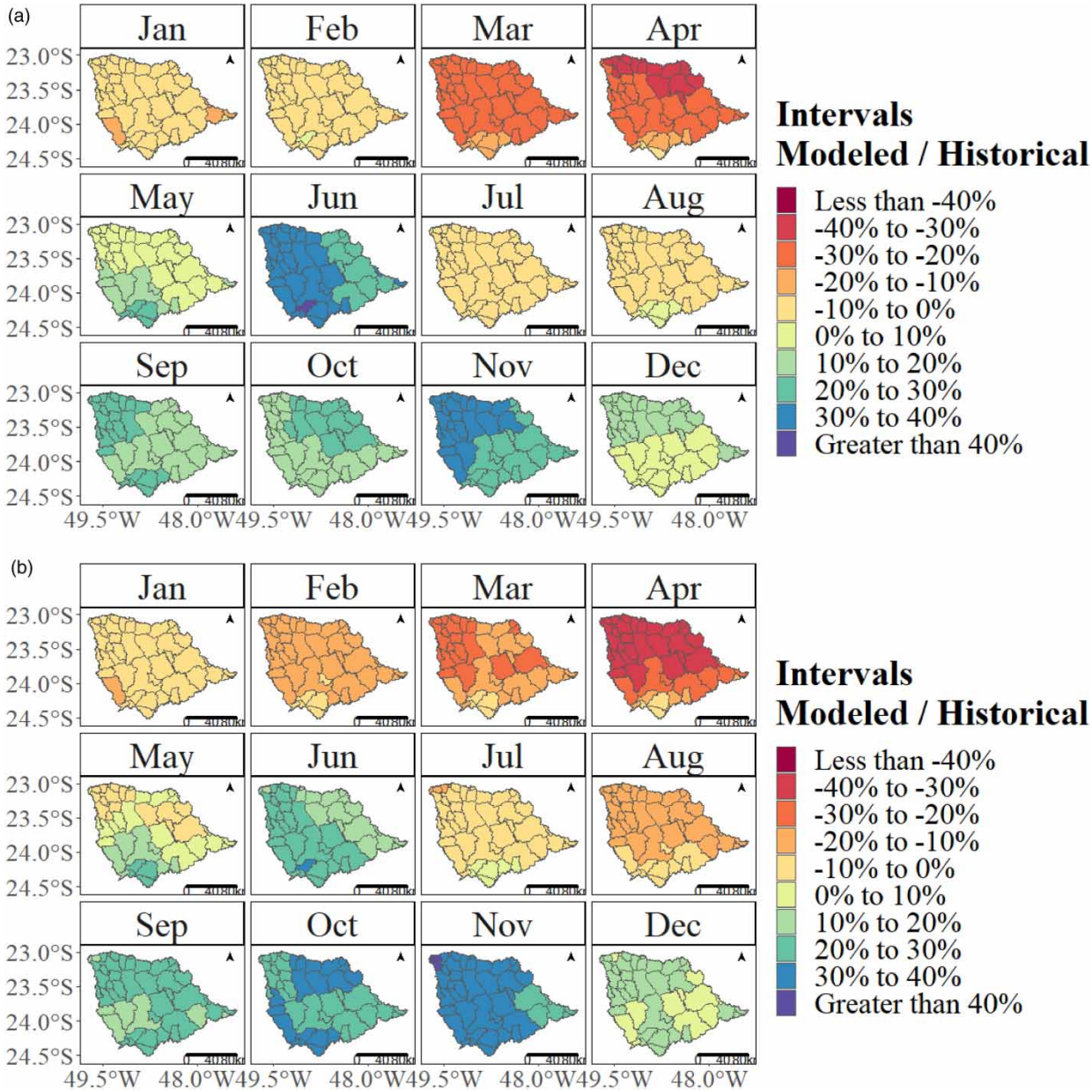

Figure 6 | Yearly rainfall variation for the Eta–Miroc climate model under the RCP 4.5 (a) and RCP 8.5 (b) scenarios.

A comparison between (a) and (b) of Figures 3–6 illustrates the impact of climate change, considering the differences between both RCP scenarios. Figure 3(b), which depicts the Eta–BESM climate model and RCP 8.5 scenario, demonstrates a more extreme scenario than that shown in Figure 3(a) (RCP 4.5 scenario). The reduction of rainfall during January through April is greater in Figure 3(b) than in the previous scenario, and the increase in rainfall during the wet season, mainly October and November, is smaller than in the RCP 4.5 scenario. These findings indicate that extreme events have a higher chance of occurring in the RCP 8.5 scenario. However, there is no significant change in rainfall during June and July.

When comparing the Eta–BESM and Eta–CanESM models, a slight increase in rainfall during the dry season and a slight decrease in rainfall during the wet season can be observed.

Comparison of the Eta–HadGEM model with the other models reveals that it combines the results of the previous two models (Eta–BESM and Eta–CanESM). Specifically, during the dry season, the Eta–HadGEM model indicates less rainfall

compared to the historical data, like the Eta–BESM model. Additionally, during the wet season, the Eta–HadGEM model shows a decrease in rainfall, although not as much as in the Eta–CanESM model.

To enhance visualization and facilitate comparison, Table 2 presents a concise summary of the findings depicted in the maps.

One of the reasons behind this contrast lies in the structural variances of the GCMs, as illustrated in Table 1, which lead to the generation of the distinct outcomes. The GCMs and the RCMs can better represent some climate zones, such as the relationship found between Eta–Miroc and the Intertropical Convergence Zone (Chou *et al.* 2014a). Furthermore, the seasonality affects the models, and the precipitation can correlate to a region in one season but not the other. An example is Eta–HadGEM, where in the December-January period it is highly correlated with the whole territory, but during the June-August period, it loses its power and is outperformed by other models (Chou *et al.* 2014a). Another remark is the different RCP scenarios. Reduction in precipitation caused by the more severe RCP 8.5 scenario can only be visualized in some models and seasons, like Eta–Miroc and Eta–HadGEM (Chou *et al.* 2014b). While previous studies have not delved into this aspect, it is highly probable that Eta–CanESM exhibits analogous behavior to the other models and demonstrates a stronger correlation with a particular region during a specific period.

The Eta–Miroc model shares a similar trend to that of other models. However, the change in rainfall when compared to the historical data is more subtle than the other models, both in the wet and dry seasons.

Three primary inferences regarding the trends in rainfall for the predicted years emerge. Firstly, there will be a general reduction in rainfall, with precipitation concentrated in fewer months during the wet season. This will result in longer and more severe droughts, which will have a significant impact on sectors such as agriculture and power generation. Furthermore, the concentration of rainfall in fewer months may lead to extreme weather events occurring more frequently. Secondly, during the dry season, there will be an increase in rainfall, which could affect the agricultural sector by altering the optimal time to begin planting crops. This change could result in crop losses and have a negative impact on the economy. Finally, the third trend predicts an increase in rainfall during the wet season, accompanied by a reduction in rainfall during the dry season. This trend may lead to frequent storms that could, e.g., damage stormwater drainage systems in cities, cause soil erosion in rural areas, and create dangerous droughts for water supply and energy generation systems.

To gain a better understanding of the impacts on society, the analysis of rainfall should be converted to river flow. The comparison of historical data provides a valuable analysis, particularly with regards to the extreme hydrological events that occurred in the late 1970 and 1980 s. When this data is converted into a line graph for the Jurumirim and Chavantes watersheds, as depicted in Figure 7, it becomes evident that there are notable spikes in river flow during this period.

The calibration and validation results were obtained for both sub-basins of the SMAP model. The model was calibrated using the optimal time series data from 1979 to 1984, while validation was performed using data from 1968 to 1973. The NSE coefficient for the calibration and validation of both sub-basin is represented in Table 3. Chavantes was calibrated using data from the Jurumirim sub-basin, as the available data from the Chavantes sub-basin alone proved insufficient for the SMAP model calibration. The weather stations used in this step were SAG, E5-030, F5-041, E5-027, E5-019, E6-013 and E6-022

Table 2 | Summary of the minimum and maximum changes in modeled rainfall over historical data (%) for RCP 4.5 (above) and RCP 8.5 (below) and all provinces together

		Eta–BESM (%)	Eta–CanESM (%)	Eta–HadGEM (%)	Eta–Miroc (%)
RCP 4.5					
Wet months	Minimum	−52	−29.5	−47.3	−32.8
	Maximum	61	36.1	24.4	38.4
Dry months	Minimum	−1.5	−25.8	−23.5	−9.9
	Maximum	232.5	43.9	9	42.6
RCP 8.5					
Wet months	Minimum	−61.5	−35.2	−49.8	−36
	Maximum	52	19.4	19.2	41.3
Dry months	Minimum	−10.9	−33	−16.8	−19.2
	Maximum	164.6	30.2	57.6	30.3

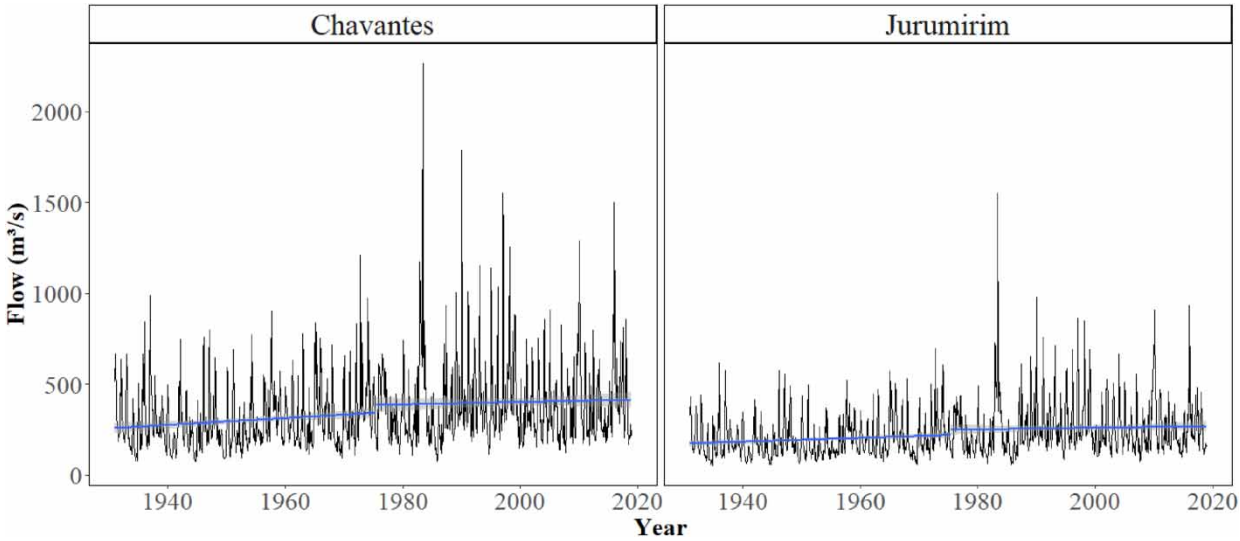

Figure 7 | Monthly river flow historical data and trend (blue lines) for the Chavantes (left) and Jurumirim (right) watersheds. A break in the trendlines is easily identified in the 1970s, from which the average rate of streamflow has diminished.

Table 3 | NSE coefficient for the calibration and validation of the SMAP model for both sub-basins

	Chavantes	Jurumirim
Calibration	0.79	0.82
Validation	0.47	0.77

As visible in Figure 7, prior to the identified break in the trendline, the river flow exhibited an annual increase, while after the break, the river flow stabilized. Had the break not been identified, the data would have suggested a steady increase in river flow over time (the average increase throughout the entire historical streamflow data). This insight highlights the potential for both positive and negative changes in river flow, without any abrupt changes on the overall streamflow behavior. Figure 8 presents a comparison between the historical and predicted river flow.

The river flow was subjected to the SMAP model using the parameters obtained during the previous calibration step, and the resulting NSE coefficients are presented in Table 4.

Interestingly, the RCP 4.5 yields a suboptimal NSE coefficient, whereas the RCP 8.5 exhibits two scenarios with positive scores. Negative values of the NSE coefficient suggest that the mean values of the observed series serve as a more effective predictor.

Located in the southwest of Brazil, both watersheds exhibit a known transient behavior that mimics a sine curve. This is a result of the watersheds location in a transition zone between the atmospheric convergence zones of the north and south (Chou *et al.* 2014a, 2014b; Utida *et al.* 2019; Wong *et al.* 2021). During the wet season, there are losses from January to March and gains from October to December, with a steep drop in the latter month. In the dry season, losses occur from April to June and gains from July to September. Overall, losses account for approximately 60% of the total, while gains can exceed 200%. As with the rainfall analysis, caution must be taken when analyzing these values to avoid misinterpretation of the river flow data.

The RCP 8.5 scenario presents a less optimistic outlook, with greater losses and less accentuated gains when compared to RCP 4.5. The Eta–Miroc model, on the other hand, shows an interesting trend in the two different scenarios, with a smaller difference between them regarding the other models. This trend can be better visualized when the data are broken down by climate normal, as shown in Figure 8(b)–8(d).

The Eta–Miroc model shows that, under the last climate normal, the RCP 8.5 exhibits a greater decrease in river flow compared to RCP 4.5, highlighting that climate change is not solely correlated with a reduction in rainfall and river flow, but also

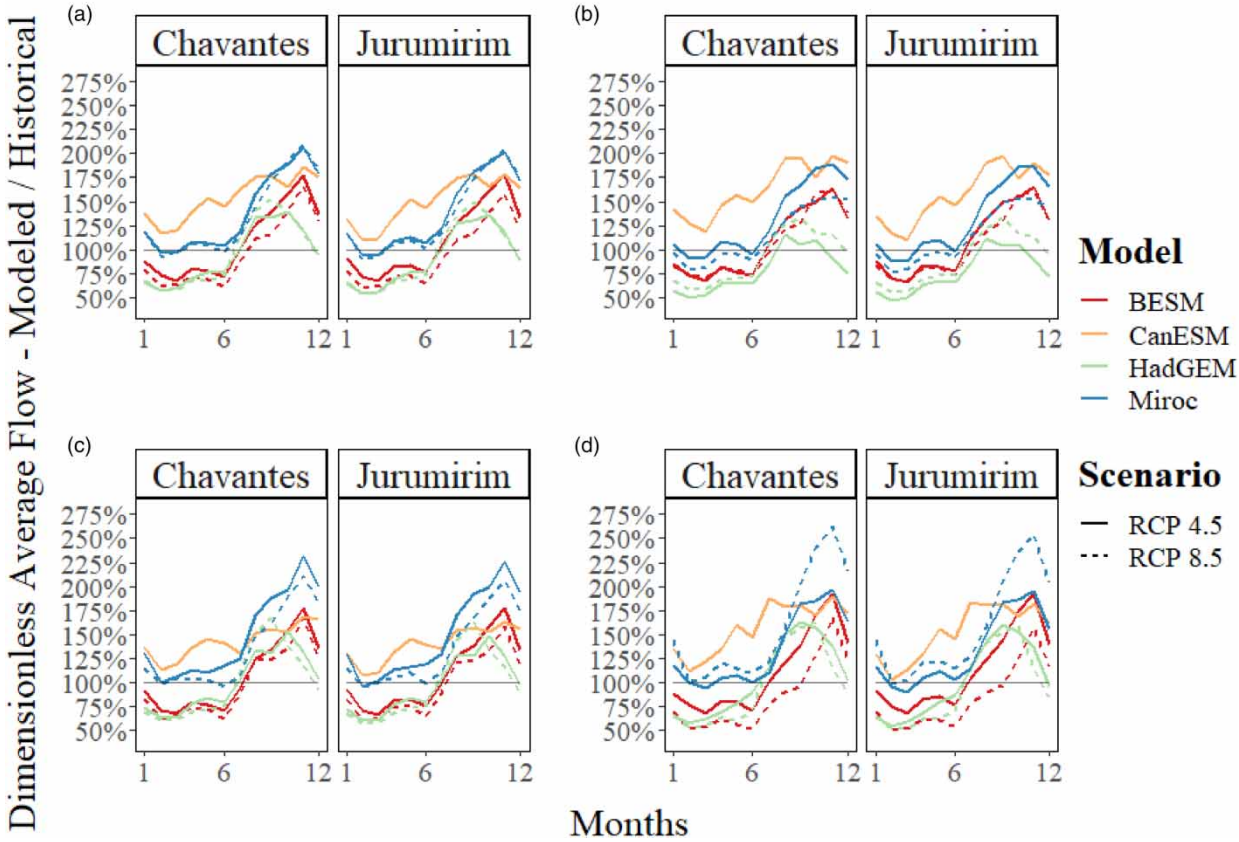

Figure 8 | Compared average river flow for Chavantes and Jurumirim watersheds from 2010 to 2099 (a), 2010 to 2039 (b), 2040 to 2069 (c), and 2070 to 2099 (d).

Table 4 | The NSE coefficient results for the SMAP model calculated for river flows in each sub-basin, considering each model and RCP scenario

Model/Scenario	Chavantes	Jurumirim
BESM4.5	0.09	−0.01
CanESM 4.5	−1.17	−0.08
HadGEM 4.5	0	0.15
Miroc 4.5	−0.68	−0.65
BESM 8.5	0.16	0.22
HadGEM 8.5	0.02	0.18
Miroc 8.5	−0.68	−0.62

with changes in the atmospheric behavior that affects the depth, timing, and location of rainfall. Even though the data is segmented into climate normal, it continues to exhibit a sinusoidal pattern akin to that shown in Figure 8. Furthermore, these results reveal a potential decrease in river flow over the next century, with the largest decrease occurring in the latter half of the period under analysis (2050–2100). To further illustrate this decline in river flow, single graphs with trend lines have been presented in Figure 9.

All trend lines point to river flow reduction, with two exceptions. First, the model Eta–HadGEM RCP 4.5, presents a slight increase in river flow. This can be attributed to a bias of this model in the study area that evidences a bigger rainfall response

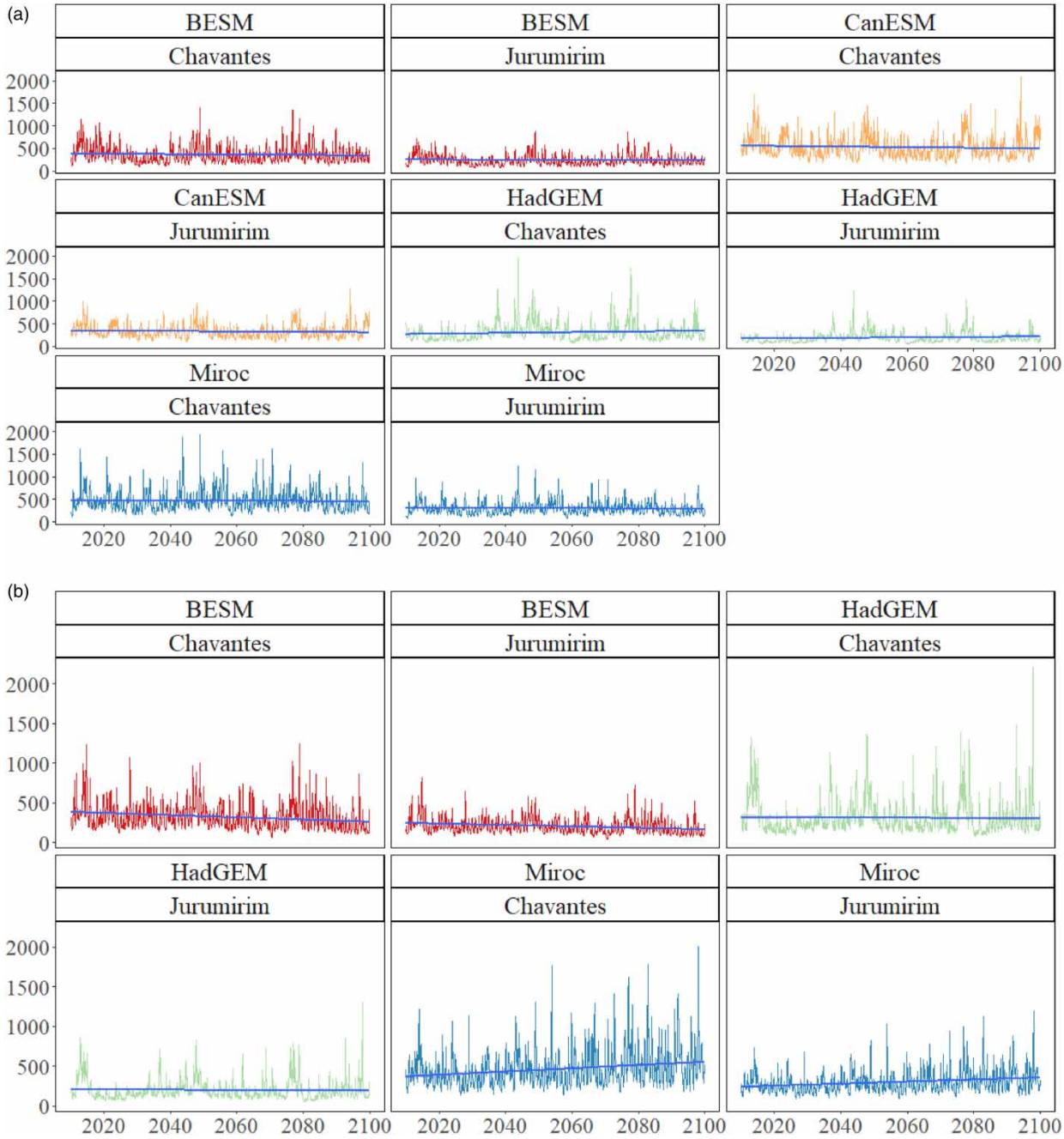

Figure 9 | Yearly predicted river flow and trend lines from 2010 to 2099 for Chavantes and Jurumirim watersheds, under the RCP 4.5 (a) and RCP 8.5 (b) scenarios.

than the other models. Secondly, the Eta–Miroc in RCP 8.5 scenario reinforces the previously discussed about trends on climate normal.

CONCLUSIONS

Climate modeling data plays an indispensable role in providing essential insights for water managers, enabling them to effectively address and mitigate the adverse consequences of climate change on societal well-being. Efficient water resource management is achieved by combining predictive models and promoting strong information exchange among basin

management units. This approach safeguards these resources for both present and future generations. This is particularly significant within the context of the ALPA Basin in the state of São Paulo, Brazil, which assumes a pivotal role as a fundamental water source across various socio-economic sectors.

The importance of proficient water resource management highlights the need for cohesive collaboration and effective communication among the entities responsible for overseeing basin dynamics. This collaborative synergy ensures a comprehensive approach to the sustainable preservation of water resources. Simultaneously, the development and implementation of predictive models assumes paramount significance. These models provide us with the foresight needed to anticipate shifts in water availability and demand, thereby empowering us to proactively adapt to evolving circumstances.

The exhaustive analysis conducted within the Chavantes and Jurumirim watersheds underscores the urgency for proactive interventions. The projected decline in water flow attributed to a multitude of factors, including growing population, escalating water consumption, and evolving land utilization patterns – notably exemplified by the proliferation of center-pivot irrigation systems – foreshadows a concerning alteration in the hydrological cycles of these basins. The ramifications extend beyond the boundaries of the studied headwater sub-basin, cascading downstream and causing disruptions across interconnected basins.

The hydrological stress in the studied region becomes evident in the marked reduction in rainfall of up to −40% during the traditionally wet months of January through April. Furthermore, the anomalous increase of rainfall of up to 40% during the dry season months of June and July, coupled with the wet season months of October and November, underscore the climate-induced modulation of historical precipitation patterns. According to the calculations, in terms of river flow, the Chavantes River witnessed its lowest historical discharge of 73 m^3/s, which would be modified to 20 m^3/s, while its highest historical flow of 2,266 m^3/s would be modified to 907 m^3/s. Similarly, for the Jurumirim sub-basin, the lowest historical river flow of 55 m^3/s would be modified to 39 m^3/s, and the highest historical flow of 1,552 m^3/s would be modified to 1,304 m^3/s. These manifestations underscore the urgency of a concerted and informed response. Amidst the predominant downward trends in river flow evidenced by this study, notable exceptions warrant discernment. The Eta–HadGEM RCP 4.5 model presents a marginal increment in river flow, ascribed to its distinctive capture of localized rainfall responses. Moreover, the Eta–Miroc model within the RCP 8.5 scenario reiterates the pivotal influence of climate normal in shaping these discernible trends.

In addition to its impacts on water flow patterns, climate change can also shift the distribution of precipitation, potentially causing difficulties for farming and other land uses within the ALPA Basin. Addressing this scenario requires stakeholders to come up with intelligent and creative adaptation plans. To tackle these issues effectively, it is important to look carefully into forecasts on rainfall and, generally, on local climate trends. With a deeper understanding, stakeholders in charge of water management can adopt and implement strategies to cope with the anticipated challenges.

ACKNOWLEDGEMENTS

The authors thank CPTEC/INPE for providing the data and collaboration and the Coordination for the Improvement of Higher Education Personnel (CAPES) of Brazil and Foundations for Supporting Research in the States of Minas Gerais (Fapemig) for supporting the Post-graduate Program. This study also had the support of Portuguese funds through Science and Technology Foundation (FCT), under the projects [grant numbers UIDB/04292/2020, UIDP/04292/2020], granted to MARE, and [grant number LA/P/0069/2020], granted to the Associate Laboratory ARNET.

DATA AVAILABILITY STATEMENT

Data cannot be made publicly available; readers should contact the corresponding author for details.

CONFLICT OF INTEREST

The authors declare there is no conflict.

REFERENCES

Barros, M. T. L., Lopes, J. E. G., Zambon, R. C., Francato, A. L., Barbosa, P. S. F. & Zanfelice, F. R. Climate Flow Forecast Model for the Brazilian Hydropower System. In: World Environmental and Water Resources Congress 2009, 2009, Kansas City. World Environmental and Water Resources Congress 2009. Reston: American Society of Civil Engineers. p. 1. DOI. https://ascelibrary.org/doi/10.1061/41036%28342%29476.

Barros, G. S. C., Castro, N. R., Machado, G. C., Almeida, F. M. S., Silva, A. F. & Fachinello, A. L. 2021 Boletim PIB do Agronegócio SãoPaulo -2020. *Centro de Estudos Avançados em Economia Aplicada (CEPEA)*. https://www.cepea.esalq.usp.br/upload/kceditor/files/Cepea_PIBdoAgro_set_Dez21.pdf

CBH-Alpa. SigRH 2023 Available from: https://sigrh.sp.gov.br/cbhalpa/apresentacao. (accessed in July of 2023).

Chou, S. C., Lyra, A., Mourão, C., Dereczynski, C., Pilotto, I., Gomes, J., Bustamante, J., Tavares, P., Silva, A., Rodrigues, D., Campos, D., Chagas, D., Sueiro, G., Siqueira, G. & Marengo, J. 2014a Assessment of climate change over south America under RCP 4.5 and 8.5 downscaling scenarios. *American Journal of Climate Change* **03** (05), 512–527.

Chou, S. C., Lyra, A., Mourão, C., Dereczynski, C., Pilotto, I., Gomes, J., Bustamante, J., Tavares, P., Silva, A., Rodrigues, D., Campos, D., Chagas, D., Sueiro, G., Siqueira, G., Nobre, P. & Marengo, J. 2014b Evaluation of the eta simulations nested in three global climate models. *American Journal of Climate Change* **03** (05), 438–454.

Commoner, B. 2020 The Closing Circle: Nature, Man, and Technology. Mineola, New York. Dover Publications Inc.

Green, T. R., Taniguchi, M., Kooi, H., Gurdak, J. J., Allen, D. M., Hiscock, K. M., Treidel, H. & Aureli, A. 2011 Beneath the surface of global change: Impacts of climate change on groundwater. *Journal of Hydrology* **405** (3), 532–560.

Gueymard, C. A. 2012 Clear-sky irradiance predictions for solar resource mapping and large-scale applications: Improved validation methodology and detailed performance analysis of 18 broadband radiative models. *Solar Energy* **86** (8), 2145–2169.

IBGE – Brazilian Institute of Geography and Statistics 2023 *Brazilian Official Data of Economics Resources*. Available from: https://ibge.gov.br/explica/pib.php/ (accessed in July of 2023).

INTERGOVERNMENTAL PANEL FOR CLIMATE CHANGE. Technical Summary. In Climate Change 2021 The Physical Science Basis. Contribution of Working Group I to the Sixth Assessment Report of the Intergovernmental Panel on Climate Change. Cambridge University Press, 2021, Cambridge, United Kingdom and New York, NY, USA, pp. 33–144.

Jackson, R. B., Carpenter, S. R., Dahm, C. N., McKnight, D. M., Naiman, R. J., Postel, S. L. & Running, S. W. 2001 Water in a changing world. *Ecological Applications: A Publication of the Ecological Society of America* **11** (4), 1027–1045.

Lopes, J. E. G. 1999 *Manual do Modelo SMAP*. https://pt.scribd.com/document/363902193/Smap-Manual.

Lopes, J. E. G., Braga, B. P. F. & Conejo, J. G. L. 1982 SMAP – A Simplified Hydrological Model. In: *Applied Modeling in Catchment Hydrology* (Singh, V. P., ed.). Water Resources Publications, Littleton, CO, USA, pp. 167–176.

Maraun, D., Wetterhall, F., Ireson, A. M., Chandler, R. E., Kendon, E. J., Widmann, M., Brienen, S., Rust, H. W., Sauter, T., Themeßl, M., Venema, V. K. C., Chun, K. P., Goodess, C. M., Jones, R. G., Onof, C., Vrac, M. & Thiele-Eich, I. 2010 Precipitation downscaling under climate change: Recent developments to bridge the gap between dynamical models and the end user. *Reviews of Geophysics* **48** (3). https://doi.org/10.1029/2009rg000314.

Nash, & Sutcliffe 1970 River flow forecasting through conceptual models part I – A discussion of principles. *Journal of Hydrology*. Available from: https://www.sciencedirect.com/science/article/pii/0022169470902556.

O'Neill, P., Entekhabi, D., Njoku, E. & Kellogg, K. 2010 Soil Moisture Active Passive (SMAP) mission: Overview. In: *2010 IEEE International Geoscience and Remote Sensing Symposium*, pp. 3236–3239.

Peng, J., Albergel, C., Balenzano, A., Brocca, L., Cartus, O., Cosh, M, H., Crow, W. T., Dabrowska-Zielinska, K., Dadson, S., Davidson, M. W. J., Rosnay, P., Dorigo, W., Gruber, A., Hagemann, S., Hirschi, M., Kerr, Y. H., Lovergine, F., Mahecha, M. D., Marzahn, P., Mattia, F., Musial, J. P., Preuschmann, S., Reichle, R. H., Satalino, S., Silgram, M., Van Bodegom, P. M., Verhoest, N. E. C., Wagner, W., Walker, J. P., Wegmüller, U. & Loew, U. 2021 A roadmap for high-resolution satellite soil moisture applications – confronting product characteristics with user requirements. *Remote Sensing of Environment* **252**. https://doi.org/10.1016/j.rse.2020.112162. (https://www.sciencedirect.com/science/article/pii/S0034425720305356).

Santos, L. D. L., Graciano, M. C., de Araújo, J. C. L., de Melo, D. P. & Martensen, A. C. 2023 Agribusiness and the search for land and water: Land use, irrigation and land structure in the Alto Paranapanema Region –São Paulo. *Estudos Geográficos: Revista Eletrônica de Geografia* **21** (3), 248–267.

Skaggs, R. W., Brevé, M. A. & Gilliam, J. W. 1994 Hydrologic and water quality impacts of agricultural drainage. *Critical Reviews in Environmental Science and Technology* **24** (1), 1–32.

Tiezzi, R. O., Vieira, N., Simões, A. F., Filho, H. F., Viana, E., Mouette, D. & Domingues, M. S. 2018 Impacts of climate change on hydroelectric power generation – a case study focused in the Paranapanema Basin, Brazil. *Journal of Sustainable Development in Africa* **11** (1), 140.

Tiezzi, R. O., Barbosa, P. S. F., Lopes, J. E. G., Francato, A. L., Zambon, R. C., Silveira, A., Menezes, P. H. B. J. & Isidoro, J. M. G. P. 2019 Trends of streamflow under climate change for 26 Brazilian basins. *Water Policy* **21** (1), 206–220.

Utida, G., Cruz, F. W., Etourneau, J., Bouloubassi, I., Schefuß, E., Vuille, M., Novello, V. F., Prado, L. F., Sifeddine, A., Klein, V., Zular, A., Viana, J. C. C. & Turcq, B. 2019 Tropical South Atlantic influence on Northeastern Brazil precipitation and ITCZ displacement during the past 2300 years. *Scientific Reports* **9** (1), 1–8.

van Vuuren, D. P., Edmonds, J., Kainuma, M., Riahi, K., Thomson, A., Hibbard, K., Hurtt, G. C., Kram, T., Krey, V., Lamarque, J.-F., Masui, T., Meinshausen, M., Nakicenovic, N., Smith, S. J. & Rose, S. K. 2011 The representative concentration pathways: An overview. *Climatic Change* **109** (1), 5.

Wigneron, J.-P., Jackson, T. J., O'Neill, P., De Lannoy, G., de Rosnay, P., Walker, J. P., Ferrazzoli, P., Mironov, V., Bircher, S., Grant, J. P., Kurum, M., Schwank, M., EMBRAPMunoz-Sabater, J., Das, N., Royer, A., Al-Yaari, A., Al Bitar, A., Fernandez-Moran, R., Lawrence, H,

Mialon, A. & Kerr, Y. 2017 Modelling the passive microwave signature from land surfaces: A review of recent results and application to the L-band SMOS & SMAP soil moisture retrieval algorithms. *Remote Sensing of Environment* **192**, 238–262.

Wong, M. L., Wang, X., Latrubesse, E. M., He, S. & Bayer, M. 2021 Variations in the South Atlantic convergence zone over the mid-to-late Holocene inferred from speleothem δ18o in central Brazil. *Quaternary Science Reviews* **270**, 107178.

Zhang, D. & Zhou, G. 2016 Estimation of soil moisture from optical and thermal remote sensing: A review. *Sensors* **16** (8). https://doi.org/10.3390/s16081308.

Zhang, X., Li, H.-Y., Deng, Z. D., Ringler, C., Gao, Y., Hejazi, M. I. & Leung, L. R. 2018 Impacts of climate change, policy and water-energy-food nexus on hydropower development. *Renewable Energy* **116**, 827–834.

First received 15 September 2023; accepted in revised form 20 March 2024. Available online 17 April 2024